RSC Advances

PAPER

Cite this: *RSC Adv.*, 2020, **10**, 5566

His18 promotes reactive oxidative stress production in copper-ion mediated human islet amyloid polypeptide aggregation†

Gengyang Huo,[a] Wenyong Chen,[a] Jianhua Wang,[a] Xinxing Chu,[ab] Wei Xu,[a] Bin Li,[b] Yi Zhang,[b] Binqian Xu[c] and Xingfei Zhou*[a]

Received 27th November 2019
Accepted 23rd January 2020

DOI: 10.1039/c9ra09943c

rsc.li/rsc-advances

Copper ions play a critical role in human islet amyloid polypeptide (hIAPP) aggregation, which has been found in more than 90% of patients with type-2 diabetes (T2D). The role of Cu(II) in the cell cytotoxicity with hIAPP has been explored in two aspects: inhibiting the formation of fibrillar structures and stimulating the generation of reactive oxygen species (ROS). In this work, we carried out spectroscopic studies of Cu(II) interacting with several hIAPP fragments and their variants as well. Electron paramagnetic resonance (EPR) measurements and Amplex Red analysis showed that the amount of H_2O_2 generated in hIAPP(11-28) solution co-incubated with Cu(II) was remarkably more than hIAPP(1-11) and hIAPP(28-37). Furthermore, the H_2O_2 level was seriously reduced when His18 of hIAPP(11-28) was replaced by Arg(R) or Ser(S), indicating that His18 is the key residue of Cu(II) binding to hIAPP(11-28) to promote H_2O_2 generation. This is likely because the donation of electrons from the peptide to Cu(II) ions would result in the formation of the redox-active complexes, which could stimulate the formation of H_2O_2. Overall, this study provides further insight into the molecular mechanism of Cu(II) induced ROS generation.

Introduction

The aggregation of amyloid peptides into supramolecular structures has been linked to more than 30 neurodegenerative disorders featured by clinically observed deposits of amyloid fibrils.[1–3] Accumulating evidence suggests that toxic deposition of human islet amyloid polypeptide (hIAPP) is one of the most common pathological features of type-2 diabetes mellitus (T2D),[4,5] characterized by chronic insulin resistance and decline in pancreatic β-cell function.[6,7] hIAPP (also named as amylin) is a peptide hormone that is initially produced by β-cells of the islet of the pancreas. It is 37 residues in length and has different functional domains including an N terminus, C terminus and the amyloidogenic central peptide sequence (residues 20-29),[8–10] which are prone to forming fibrils. The aggregation process of hIAPP has been proved to be modulated by many factors including pH value, metal ions, small chemical molecules, *etc.*[11–15]

Copper ions are believed to be closely associated with T2D as clinical findings show that the serum copper ions levels are higher in diabetic patients than in healthy people.[16,17] Recently, the particular role of copper ions in diseases associated with hIAPP aggregation has been studied extensively.[18–21] These researches have demonstrated that the presence of Cu(II) could result in the formation of oligomers or oligomer-like structures instead of fibrillar forms.[22] Particularly, Lee and co-workers showed that Cu(II)-containing intermediate species of hIAPP formed more toxic aggregates with random coil conformations.[23]

On the other hand, the binding of redox-active Cu(II) to the amyloid peptide could form the peptide–copper complexes, which can stimulate the production of ROS in a toxicity manner.[24–26] The resulting ROS, such as H_2O_2 and $OH^{\bullet}$ would damage DNA, lipids and proteins and thus trigger apoptotic cell death. While some studies report that the Cu(II)–hIAPP complexes produce hydrogen peroxide to a lesser extent than free Cu(II) in solution, suggesting the sacrificial protective roles for hIAPP coexisted with Cu(II) in high concentration.[27,28] Therefore, despite such extensive studies associated with hIAPP aggregation, the underlying mechanism of Cu(II) promoting the generation of ROS still remains obscure.

In order to clarify the mechanism of Cu(II) promoting the generation of ROS, in this study the interaction of Cu(II) with hIAPP was explored using different spectroscopy techniques. hIAPP(11-28) fragment was used as a main model, as it contains the region (20-28) for amyloid formation as well as the main binding site (His18) for the metal ions.[10,13,29] We first compared the amount of H_2O_2 production in several fragments co-

[a]School of Physics Science and Technology, Ningbo University, China. E-mail: zhouxingfei@nbu.edu.cn

[b]Shanghai Advanced Research Institute, Chinese Academy of Sciences, China

[c]Single Molecule Study Laboratory, College of Engineering, University of Georgia, Athens, Georgia 30602, USA

† Electronic supplementary information (ESI) available. See DOI: 10.1039/c9ra09943c

incubated with copper ions including hIAPP(1-11), hIAPP(11-28), hIAPP(28-37) and two variants (hIAPP(11-28, H18R) and hIAPP(11-28, H18S)). Since rat IAPP (rIAPP) differs from hIAPP in only six amino acid residues, therefore, we further evaluated the amount of H_2O_2 produced in rIAPP in the presence of Cu(II). Our results unambiguously indicate that His18 plays a central role in stimulating H_2O_2 generation during the process of hIAPP fibrillation.

Materials and methods

Materials

All synthetic human and rat IAPP/amylin fragments (hIAPP(1-11), hIAPP(11-28), hIAPP(28-37), and rIAPP(11-28)) and two variants (hIAPP(11-28, H18R) and hIAPP(11-28, H18S)) with the purity greater than 95% were purchased lyophilized from GLS, Biochem, China. Thioflavine T (ThT) was purchased from Sigma-Aldrich, China. DMPO (Dojindo, Japan) was obtained from Dongren chemical technology (Shanghai) Co. Ltd, China. The Amplex Red (Santa Cruz Biotechnology, USA) was obtained from Hangjing Biotechnology Co. Ltd, China. Metal chelator diethylenetriaminepentaacetic acid (DETAPAC) was obtained from Macklin Biotechnology technology (Shanghai) Co. Ltd, China. The Milli-Q water with a resistivity of 18.2 MΩ cm^{-1} was used in our experiments.

Amplex Red assay

A Fluoroskan ascent fluorescence spectrophotometer (Thermo Scientific Inc., USA) was used to measure the kinetics of H_2O_2 accumulation progress. For the Amplex Red assays,[30] a 10 mM stock solution of Amplex Red was prepared by dissolving 2.57 mg Amplex Red in 1 ml DMSO; 10 U ml^{-1} HRP stock solution was prepared by dissolving 10 μg HRP in 1 ml PBS (both stored in −20 °C). To obtain Amplex Red working solution, the stock HRP solution was diluted to 1/1000 in PBS and this dilute HRP solution (40 μl) and Amplex Red stock solution (20 μl) were added into PBS (940 μl). To prepare samples for fluorescence, various metal ions with hIAPP fragments at different concentrations and 50 μM Amplex Red working solution were added in 96-well microtitre plate (Corning Inc., USA). In some contrast experiments, 100 μM DETAPAC was added prior to incubation of the peptide solutions. At least four set of measurements were carried out for each tested sample. And the final results were averaged.

Electron paramagnetic resonance spectroscopy (EPR)

Electron paramagnetic resonance (EPR) spectrometer (Bruker Inc., Germany) was used to measure the hydroxyl radical during the incubation of peptide with various metal ions in PBS at 37 °C, as described previously.[31] The method employed the reaction of this radical with the spin trap 5,5-dimethyl-1-pyrroline N-oxide (DMPO) to form the hydroxyl radical adduct (DMPO–OH), which has a unique characteristic 4-line EPR spectrum. According to the Amplex Red measurement, the amount of hydrogen peroxide almost reached the peak value. Therefore, EPR measurement was performed after 50 hours incubation in order to obtain strong EPR signal. Briefly, 100 μM hIAPP or rIAPP fragments and 50 μM Cu(II) were incubated for 50 hours at 37 °C, then we added DMPO to the incubated peptide solution. And finally sample was put into the EPR equipment for measurement after full shaking.

AFM measurements

100 μM peptide fragments with and without $CuCl_2$ at different concentration (pH: 7.0) was co-incubated at 37 °C for three days, respectively, since ThT fluorescent intensity reached maximum value and kept stable after three days incubation. Then about 3–5 μl incubated solution was deposited onto freshly cleaved mica, waited for about 5 min, gently rinsed with Milli-Q water and dried in air. Images were collected using scanning probe microscope (Multimode 8, Bruker, Germany) operated in tipping mode in air. Tips used were NSC11 (Mikromash company) with a resonance frequency of ∼330 kHz and a spring constant of ∼30 N m^{-1}. All images were simply flattened using the NanoScope analysis software.

X-ray absorption fine structure (XAFS) spectra

XAFS measurements were performed at Shanghai Synchrotron Radiation Facility (SSRF) beamline BL14W. A Si[111] double crystal monochromator and a set of focusing mirrors with a cut-off energy of 22.5 keV were used throughout the study. The XAFS spectra were measured in fluorescence mode using a 32-element Ge solid-state detector. Data collected in each run were first averaged after background subtraction. To prepare a sample for XAFS measurement, 1500 ml of 200 μM hIAPP(11-28) peptide with 1000 μM $CuCl_2$ was incubated at 37 °C for three days. In order to increase the signal/noise ratio in XAFS data, each of these samples was further concentrated to 300 ml by freeze drying.

Results and discussion

We first used Amplex Red method to evaluate the effects of Cu(II) on the amount of H_2O_2 generated during an incubation of 100 μM hIAPP(11-28) with Cu(II) at different concentrations. Previous reports stated that Amplex Red fluorescence intensity is proportional to the level of produced H_2O_2.[32] Therefore, in this study we used fluorescence intensity to describe the level of H_2O_2. Fig. 1a shows that H_2O_2 increased rapidly during the early stage of hIAPP(11-28) aggregation when the concentration of copper ions was greater than 25 μM. A similar phenomena was also observed for Aβ peptide, where Huang *et al.* suggested that Cu(II) bound Aβ could generate H_2O_2.[33] In contrast, much less H_2O_2 was detected at a lower Cu(II) concentration (below 10 μM). Obviously, the rate of H_2O_2 production increased with an increase of copper concentration. Two factors may attribute to this observation, the first being that Cu(II) directly reacts with the peptide, and the secondly being the only Cu(II) available to convert it to hydroxyl radicals. When H_2O_2 concentration reached a maximum value after around 72 h incubation it declined rather rapidly to background level at longer incubation times, similar to the reports by Masad *et al.*[30] We further

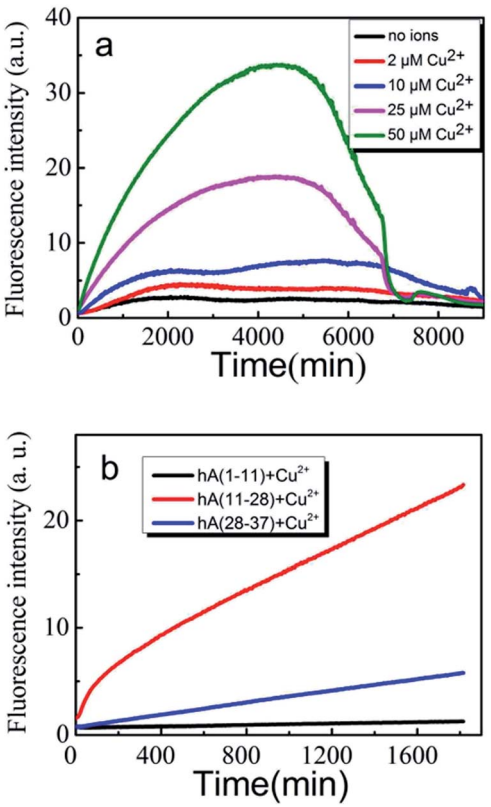

Fig. 1 H_2O_2 generation monitored by Amplex Red method. (a) 100 μM hIAPP(11-28) was incubated at 37 °C in the absence (black) and presence of 2 (red), 10 (blue), 25 (magenta) and 50 μM (olive) Cu(II). (b) 100 μM three different fragments hIAPP(1-11) (black), hIAPP(11-28) (red) and hIAPP(28-37) (blue) was co-incubated with 50 μM Cu(II) at 37 °C, respectively.

compared the level of H_2O_2 generated during the incubation of hIAPP(1-11) and hIAPP(11-28) with hIAPP(28-37) in the presence of 50 μM copper ions. As shown in Fig. 1b, Amplex Red fluorescence intensity increased rapidly for 100 μM hIAPP(11-28). In sharp contrast, the fluorescence signal only increased at a very slow speed in the case of hIAPP(1-11) and hIAPP(28-37) at the same concentration, strongly suggesting that Cu(II) specifically bind the residues located within hIAPP(11-28) and that facilitates the H_2O_2 generation.

We then employed EPR to further compare the amount of H_2O_2 generated during the incubation of three hIAPP fragments in the presence of 50 μM Cu(II). This method employed a reaction of the radical with the spin trap 5,5-dimethyl-1-pyrroline N-oxide (DMPO) to form the hydroxyl radicals.[30] As shown in Fig. 2a, the 4-line spectrum corresponding to the hydroxyl radical adduct was clearly observed for hIAPP(11-28). Remarkably, the intensity of this 4-line spectrum from hIAPP(11-28) was greater than that from hIAPP(1-11) and hIAPP(28-37), agreeing with the above Amplex Red analysis (Fig. 1b). Moreover, all of the EPR spectra obtained from hIAPP fragments could be blocked in the presence of 150 UM glutamine (data not shown), a well-known reductant. In both EPR and Amplex Red approaches, any positive signal from hIAPP was always blocked by the addition of metal chelator (DETAPAC) as shown in Fig. S1.† Our data clearly indicates that hIAPP(11-28) is the key fragment for copper ions binding to stimulate ROS production.

Finally, we probed the ultrastructures of the peptide fragment aggregates and the aggregation kinetics. Fig. 3 shows the typical AFM images of the aggregates formed when 100 μM hIAPP(11-28) was co-incubated with and without Cu(II) at different concentrations. Clearly, fibrosis progress of hIAPP was remarkably restrained by Cu(II), which was in agreement with ThT fluorescence measurement (Fig. S2†). During this incubation, the hydrogen peroxide was also generated. When hIAPP(11-28) was co-incubated with other metal ions such as Ni(II), Fe(III) and Zn(II), no detectable H_2O_2 was obtained (Fig. S3†), suggesting that Cu(II) plays a predominate role in stimulating H_2O_2 generation.

As early studies have pointed out that His18 plays a key role in modulation of hIAPP fibrillation because its ionization state significantly affects the rate of assembly and morphology of the aggregates. Thus we speculate that the generation of the H_2O_2 when hIAPP(11-28) was incubated with copper ions is likely to be associated with His18. To confirm that the His18 indeed acts as radical promoter, two variants, hIAPP(11-28, H18R) and hIAPP(11-28, H18S) were prepared. H_2O_2 level from these two variants was monitored under the same experimental condition as before. Because the residues R is positive charged and S is uncharged, thus they are not prone to combine with copper ions. Fig. 2b and 4a clearly show that the amount of H_2O_2

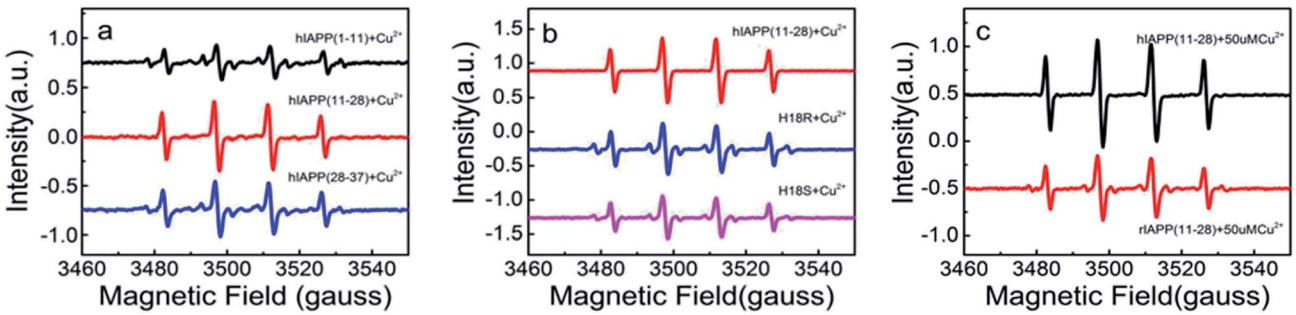

Fig. 2 Hydroxyl radical EPR signal (DMPO spin trap) induced by Cu(II) on different hIAPP fragments and variants. (a) 100 μM hAPP(1-11), hAPP(11-28) or hAPP(28-37) co-incubated with 50 μM Cu(II), respectively. (b) Comparison of hIAPP(11-28) with two variants (hIAPP(11-28, H18R) and hIAPP(11-28, H18S)). (c) Comparison of rIAPP(11-28) with hIAPP(11-28) in the presence of Cu(II).

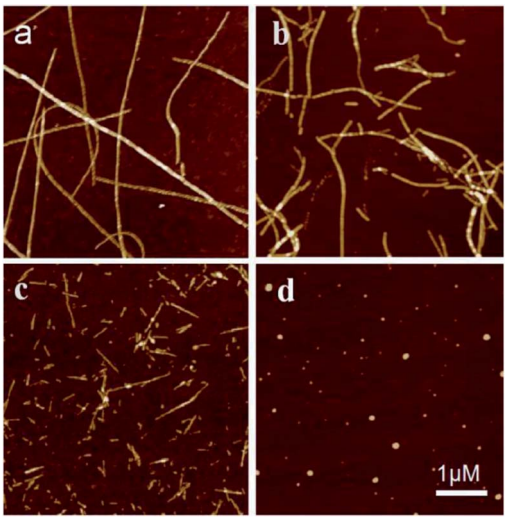

Fig. 3 AFM images of 100 μM hIAPP(11-28) incubated at 37 °C for three days in the absence and presence of copper ions at different concentrations. (a) Incubated alone. (b) 10 μM, (c) 50 μM and (d) 100 μM.

produced in hIAPP(11-28) is obviously more than that in two mutation samples. Moreover, the sequence differences between human and rat IAPP are the substitution of His18 by Arg in rat and the presence of three Pro residues within the region of 20-29. Therefore, we explored the H_2O_2 value produced during the incubation of 50 μM Cu(II) with 100 μM rIAPP(11-28), which is unable to form fibrils (Fig. S4†). Both Amplex Red signal and the 4-line peak intensity show that H_2O_2 level in rIAPP is significantly lower than in hIAPP(11-28) (Fig. 2c and 4b).

It has been reported that Cu(II) could inhibit the aggregation of hIAPP,[18,24,34] it is likely because Cu(II) anchors to His18. In fact, His18 could also be an anchoring residue for Zn(II), Ni(II), Fe(III) and even ruthenium complexes, each of them described as inhibitors of IAPP amyloid aggregation.[17,35,36] However, when hIAPP(11-28) was co-incubated with Zn(II), Fe(III) or Ni(II) ions, there was no detectable H_2O_2 production (Fig. S3†). Therefore, we used X-ray absorption fine structure (XAFS) spectroscopy to evaluate the chemical structure of Cu(II) in the peptide solution.[37] Fig. 5 suggests that Cu(II) could probably be reduced to Cu(I) upon binding to hIAPP(11-28), resulting in a hIAPP–Cu(I) complex. The major peak of the spectrum for copper ions in the hIAPP(11-28) solution was clearly observed at the same location as the peak of Cu(II) in the $CuCl_2$ solution (8995.7 eV),[38] suggesting that most of the copper ions in the hIAPP solution stay in solution. Particularly, a shoulder peak appeared in the left region of the major peak. To present the location of this minor peak clearly and exactly, the derivative was performed over the spectrum, and a zero value corresponding to the shoulder peak was clearly observed at about 8982.5 eV, which was very close to the location 8981.6 eV of Cu(I) in the Cu_2O solution,[39,40] indicating the presence of cuprous ions in the sample, following by the formation of the hIAPP–Cu(I) complexes. This results agreed well with the previous assumption that the donation of electrons from the peptide to Cu(II) ions would result in the

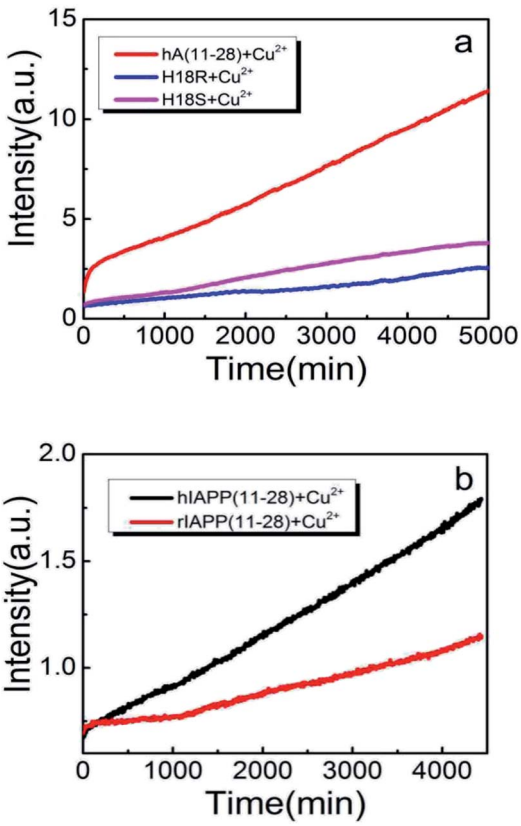

Fig. 4 H_2O_2 formation monitored by Amplex Red method. (a) 100 μM hIAPP(11-28) incubated with Cu(II), compared with two variants (hIAPP(11-28, H18S) and hIAPP(11-28, H18R)). (b) 100 μM hIAPP(11-28) or rIAPP(11-28) co-incubated with 50 μM Cu(II).

formation of Cu(I)–peptide complexes.[30] We speculate that the formed Cu(I)–peptide complexes thus catalyzed the formation of H_2O_2 as observed in our experiment.

Although it has been established previously that exposure to the hIAPP increases H_2O_2 levels in cultured cells. Our results showed that the formation of H_2O_2 in this way is selectively stimulated by Cu(II) ions. The interaction between hIAPP and the Cu(II) ions examined by EXAFS suggests possible binding of

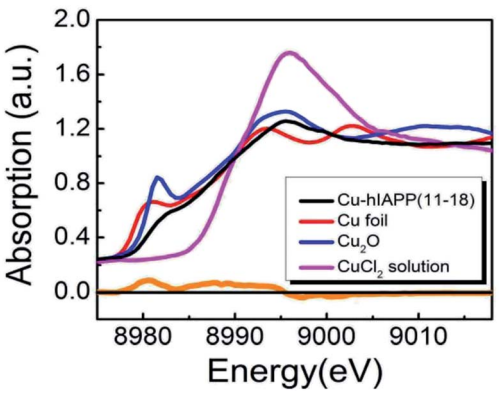

Fig. 5 XAFS spectra of the copper ions in hIAPP(11-28) solution. The orange curve represents the derivative of the Cu–hIAPP spectrum.

Cu(II) ions to hIAPP to promote the production of hydrogen peroxide. The formation of H_2O_2 could explain the well-established toxicity of this peptide towards islet cells, which in agree well with the previous reports that the cytotoxicity induced by hIAPP involves oxidative damage.[41]

Conclusions

In summary, we used several different spectroscopy approaches to study the effects of Cu(II) on hIAPP(11-28) peptide aggregation. The Amplex Red analysis and EPR results show that Cu(II) could promote the production of H_2O_2 when hIAPP(11-28) was co-incubated with Cu(II). His18 is the key event of copper ions binding to hIAPP to produce H_2O_2. Our XAFS data indicate that the binding of Cu(II) to hIAPP would potentially lead to the formation of the redox-active complexes that could stimulate the formation of H_2O_2. Among several neurodegenerative diseases commonly found in humans, particularly T2D, the facilitation of ROS formation from amyloid peptide in the presence of the oxidizing metal ions could possibly account for vivo damage to the pancreas in T2D.[41] Our research could thus provide a new insight into molecular mechanism on Cu(II) induced ROS generation, which are significantly involved in amyloid toxicity, and even the development of drug design for type-2 diabetes and other diseases.

Conflicts of interest

There are no conflicts to declare.

Acknowledgements

This work is funded by the National Natural Science Foundation of China (11474137, 11674344, 31670871), the Natural Science Foundation of Zhejiang, China (LY18A040003), the Natural Science Foundation of Ningbo, China (2018A610220) and the K. C. Wong Magna Fund in Ningbo University.

Notes and references

1 C. Soto, *Nat. Rev. Neurosci.*, 2003, **4**, 49–60.
2 P. C. Ke, M. A. Sani, F. Ding, A. Kakinen, I. Javed, F. Separovic, T. P. Davis and R. Mezzenga, *Chem. Soc. Rev.*, 2017, **46**, 6492–6531.
3 M. Ahmed, J. Davis, D. Aucoin, T. Sato, S. Ahuja, S. Aimoto, J. I. Elliott, W. E. Van Nostrand and S. O. Smith, *Nat. Struct. Mol. Biol.*, 2010, **17**, 561–567.
4 P. Faller, C. Hureau and G. La Penna, *Acc. Chem. Res.*, 2014, **47**, 2252–2259.
5 R. L. Hull, G. T. Westermark, P. Westermark and S. Kahn, *J. Clin. Endocrinol. Metab.*, 2014, **89**, 3629–3643.
6 A. Mukherjee, D. Morales-Scheihing, P. C. Butler and C. Soto, *Trends Mol. Med.*, 2015, **21**, 439–449.
7 H. R. Jeong and S. S. An, *Clin. Interv. Aging*, 2015, **10**, 1873–1879.
8 P. Westermark, A. Andersson and G. T. Westermark, *Physiol. Rev.*, 2011, **91**, 795–826.
9 A. I. Ilitchev, M. J. Giammona, T. D. Do, A. G. Wong, S. K. Buratto, J. Shea, D. P. Raleigh and M. T. Bowers, *J. Am. Soc. Mass Spectrom.*, 2016, **27**, 1010–1018.
10 A. Magrì, A. Pietropaolo, G. Tabbì, D. La Mendola and E. Rizzarelli, *Chem.–Eur. J.*, 2017, **23**, 17898–17902.
11 A. S. DeTomaa, S. Salamekha, A. Ramamoorthya and M. H. Lim, *Chem. Soc. Rev.*, 2012, **41**, 608–621.
12 L. Ghalebani, A. Wahlström, J. Danielsson, S. K. T. S. Wärmländer and A. Gräslund, *Biochem. Biophys. Res. Commun.*, 2012, **421**, 554–560.
13 M. Alghrably, I. Czaban, Ł. Jaremko and M. Jaremko, *J. Inorg. Biochem.*, 2019, **191**, 69–76.
14 J. Wu, J. Zhao, Z. Yang, H. Li and Z. Gao, *Chem. Res. Toxicol.*, 2017, **30**, 1711–1719.
15 J. Guo, W. Sun, L. Li, F. Liu and W. Lu, *RSC Adv.*, 2017, **7**, 43491–43501.
16 T. Naka, H. Kaneto, N. Katakami, T. Matsuoka, A. Harada, Y. Yamasaki, M. Matsuhisa and I. Shimomura, *Endocr. J.*, 2013, **60**, 393–396.
17 F. Bozkurt, R. Tekin, S. Gulsun, Ö. Satıcı, O. Deveci and S. Hosoglu, *Int. J. Diabetes Dev. Ctries.*, 2013, **33**, 165–169.
18 B. Ward, K. Walker and C. Exley, *J. Inorg. Biochem.*, 2008, **102**, 371–375.
19 M. Seal and S. G. Dey, *Inorg. Chem.*, 2018, **57**, 129–138.
20 K. J. Barnhamabc and A. I. Bush, *Chem. Soc. Rev.*, 2014, **43**, 6727–6749.
21 X. Dong, T. Svantesson, S. B. Sholts, C. Wallin, J. Jarvet, A. Graslund and S. K. T. S. Wärmländer, *Biochem. Biophys. Res. Commun.*, 2019, **510**, 520–524.
22 Y. Yu, P. Lei, J. Hu, W. Wu, Y. Zhao and Y. Li, *Chem. Commun.*, 2010, **46**, 6909–6911.
23 S. J. C. Lee, T. S. Choi, J. W. Lee, H. J. Lee, D. Mun, S. Akashi, S. Lee, M. H. Lim and H. I. Kim, *Chem. Sci.*, 2016, **7**, 5398–5406.
24 L. Ma, X. Li, Y. Wang, W. Zheng and T. Chen, *J. Inorg. Biochem.*, 2014, **140**, 143–152.
25 C. Cheignon, M. Tomas, D. Bonnefont-Rousselot, P. Fallerf, C. Hureau and F. Collin, *Redox Biol.*, 2018, **14**, 450–464.
26 A. Magrì, D. La Mendola, V. G. Nicoletti, G. Pappalardo and E. Rizzarelli, *Chem.–Eur. J.*, 2016, **22**, 1–15.
27 J. T. Pedersen, S. W. Chen, C. B. Borg, S. Ness, J. M. Bahl, N. H. H. Heegaard, C. M. Dobson, L. Hemmingsen, N. Cremades and K. Teilum, *J. Am. Chem. Soc.*, 2016, **138**, 3966–3969.
28 E. C. Lee, E. Ha, S. Singh, L. Legesse, S. Ahmad, E. Karnaukhova, R. P. Donaldsona and A. M. Jeremic, *Phys. Chem. Chem. Phys.*, 2013, **15**, 12558–12571.
29 L. Rivillas-Acevedo, C. Sánchez-López, C. Amero and L. Quintanar, *Inorg. Chem.*, 2015, **54**, 3788–3796.
30 A. Masad, L. Hayes, B. J. Tabner, S. Turnbull, L. J. Cooper, N. J. Fullwood, M. J. German, F. Kametani, O. M. El-Agnaf and D. Allsop, *FEBS Lett.*, 2007, **581**, 3489–3493.
31 S. Turnbull, B. J. Tabner, O. M. A. El-Agnaf, S. Moore, Y. Davies and D. Allsop, *Free Radic. Biol. Med.*, 2001, **30**, 1163–1170.

32 S. Miwa, A. Treumann, A. Bell, G. Vistoli, G. Nelson, S. Hay and T. von Zglinicki, *Free Radic. Biol. Med.*, 2016, **90**, 173–183.
33 X. Huang, C. S. Atwood, M. A. Hartshorn, G. Multhaup, L. E. Goldstein, R. C. Scarpa, M. P. Cuajungco, D. N. Gray, J. Lim, R. D. Moir, R. E. Tanzi and A. I. Bush, *Biochem*, 1999, **38**, 7609–7616.
34 A. Sinopoli, A. Magrì, D. Milardi, M. Pappalardo, P. Pucci, A. Flagiello, J. J. Titman, V. G. Nicoletti, G. Caruso, G. Pappalardo and G. Grasso, *Metallomics*, 2014, **6**, 1841–1852.
35 J. R. Brender, K. Hartman, R. P. R. Nanga, N. Popovych, R. de la Salud Bea, S. Vivekanandan, E. N. G. Marsh and A. Ramamoorthy, *J. Am. Chem. Soc.*, 2010, **132**, 8973–8983.
36 L. Ma, Y. Fu, L. Yu, X. Li, W. Zheng and T. Chen, *RSC Adv.*, 2015, **5**, 17405–17412.
37 E. De Santis, E. Shardlow, F. Stellato, O. Proux, G. Rossi, C. Exley and S. Morante, *Condens. Matter*, 2019, **4**, 13.
38 H. Yi, G. Zhang, J. Xin, Y. Deng, J. T. Miller, A. J. Kropf, E. E. Bunel, X. Qi, Y. Lan, J. F. Lee and A. Lei, *Chem. Commun.*, 2016, **52**, 6914–6917.
39 V. A. Streltsov, R. S. K. Ekanayake, S. C. Drew, C. T. Chantler and S. P. Best, *Inorg. Chem.*, 2018, **57**, 11422–11435.
40 D. Witkowskaa and M. Rowińska-Żyrek, *J. Inorg. Biochem.*, 2019, **199**, 1–10.
41 S. Zraika, R. L. Hull, J. Udayasankar, K. Aston-Mourney, S. L. Subramanian, R. Kisilesky, W. A. Szarek and S. E. Kahn, *Diabetologia*, 2009, **52**, 626–635.